

Dissipative structure formation in cold-rolled Fe and Ni during heavy ion irradiation

P. Sen, G. Aggarwal and U. Tiwari

School of Physical Sciences, Jawaharlal Nehru University, New Delhi-110067, India

We report 4-probe resistivity measurements of cold-rolled Ni and Fe during 100 MeV oxygen ion irradiation, at 300K. The resistivity shows increase and saturation, marked by jumps. Employing 200 MeV silver ion irradiation of Fe and Si(100) and topographically identifying strain at an artificial interface in the latter, we assign the resistivity behavior to atomic rearrangements arising from dissipation of incident ion energy at internal interfaces of Ni and Fe, with positive feedback.

PACS: 61.80.Jh, 61.10.Nz, 61.72.Cc

Dissipative processes lead to various mechanisms of energy storage and their release in natural systems. Development of dissipative structures in time and space are therefore a well studied phenomenon [1-3]. Recently, formation of such structures in time have been theoretically predicted in metals under ion irradiation [1]. Here the irradiating ions provide a radiation damage energy, which is stored. The resulting periodic oscillations of temperature and defect concentration are seen to originate from two competing processes: (1) defect formation during irradiation and (2) defect recombination. The latter produces heat which initiates further recombination through enhanced defect mobility. Under favourable conditions, oscillations set in as a result of this feedback.

According to established principles of energy transfer during ion irradiation, defects are introduced in a material directly by displacement of the lattice atoms and indirectly through de-excitation of the electronic subsystem. However at high energy (\sim several MeV), achieved by accelerating heavy ions, the above regions of energy transfer can be spatially separated. With thin specimens, processes initiated purely by energy transfer to lattice electrons and their subsequent de-excitation can be investigated. Such processes are called electronic energy loss or electronic stopping (S_e) initiated as the ions lose energy through excitation of lattice electrons.

It is now established that structural modifications introduced by electronic loss in a material range from displacive phase transitions in Ti to track formation in NiZr₂ alloys and metallic glasses [4-6]. While lattice defects and track formation take place above a certain threshold, phase transformations can be a sub-threshold phenomenon. Some metals like Fe, Co and Zr have also been found to be sensitive to S_e [7], forming point defects above threshold, while short range order modification is observed in austenitic alloys [8]. In general, metals showing various allotropic phases are seen to be prone to defect forma-

tion and change of phase. In the case of free surfaces and interfaces, mixing takes place irrespective of the material's sensitivity to S_e in the bulk. Such systems reported are multilayers of crystalline Ni/Ti, amorphous Si/Fe and amorphous W/Si [8,9].

Thus a possibility of dissipating electronic loss energy through atomic displacements exists, which under favourable conditions, could lead to dissipative structure formation. In this Letter we first show experimental evidence of features in a 4-probe resistivity measurement in Fe and Ni, under irradiation, which we assign to formation of such structures. We show their behavior when scaled with specimen temperature, ion flux, sampling current, S_e and metallic microstructure. The process leading to the formation of dissipative structures is established by a novel experiment employing x-ray topographic (XRT) analysis of strain developed across an ion irradiated interface, artificially generated in a single crystal. The results are extended to polycrystalline Ni and Fe which are looked upon as "single crystals" with internal surfaces. The very nature of the measurement allowed us to record the entire sequence of energy storage and release in one single experiment. To the best of our knowledge, this is the first such observation in a metal.

Resistivity measurements were computer controlled to operate a 4-probe setup where 10 μm foils (15 mm long; cold rolled and 99.99% pure from Goodfellow, UK) were attached to a constant flow cryostat and irradiated in a selected region, 5 mm wide, between the inner pair of voltage probes, while a pair of outer probes supplied constant sampling current (I). The metallic samples are assumed to be affected predominantly by S_e , as the irradiating ion range, R , is larger than the sample thickness. The relevant parameters calculated for 100 MeV oxygen irradiation of Ni (O/Ni) and Fe (O/Fe) are $R_{\text{O/Ni}} = 33 \mu\text{m}$ and $R_{\text{O/Fe}} = 37 \mu\text{m}$ respectively. For both these systems the estimated ion energy loss (average values for O/Ni and O/Fe are 2.25 and

2 MeV/ μm respectively) due to electronic means in the 10 μm thick samples is above 99%, calculated employing standard techniques [10].

The response voltage (RV), generated during irradiation of Fe and Ni at 300K with 100 MeV oxygen ions, in presence of various currents I , is presented in Fig.1. The irradiation time, t , is in terms of steps, each of 0.2 sec duration so that $t = 0$ corresponds to the time an ion beam was switched on. The beam-off positions are aligned to $t = 380$ for Ni and $t = 249$ for Fe. A general feature characterising the behavior of RV with irradiation time is the following: (1) Rise in RV during irradiation and subsequent progress in attaining a steady state, where RV does not vary considerably and (2) when the irradiating ions are removed, RV drops within seconds, to its pre-irradiated value. We record two inferences at this point. Firstly, the changes in RV are typical of defect formation during irradiation and their subsequent annihilation in absence of the ions. And secondly, RV increases and decreases in jumps (defined as a discontinuous rise or fall in voltage of the order of 10^{-6} V) whose number has a sampling current dependence. The inset to both the figures show these jumps. The jumps are random in nature and disappear when RV reaches saturation. But RV, during irradiation, does not scale with I .

We shall now establish the nature of dissipative processes operative in the above experiment. It is known that polycrystalline materials, similar to the ones employed for the experiment described above, contain grain boundaries separating individual “single crystal” grains from each other. The internal periodicity of an individual grain is lost at the grain boundary. In order to study its ion irradiation behavior we artificially create an irradiated/unirradiated interface (called irradiation interface henceforth) in a perfect single crystal of Si which is investigated for strain, employing XRT. In XRT, a reciprocal lattice vector \vec{g} is chosen so that incident x-rays suffer Bragg diffraction $\vec{K}_g = \vec{K} + \vec{g}$, while a lattice strain vector \vec{b} modifies the scattered x-ray distribu-

tion. The relative orientation of \vec{g} and the lattice strain vector \vec{b} provides for the intensity selection rule $\vec{g} \cdot \vec{b} = 0$. The crystal surface is then mapped to provide a picture of the strain developed at the interface. The technical details have already been published [11].

In Fig.2 we present results obtained from our XRT analysis. The irradiation interface is constructed by employing a masking grid, schematically presented in Fig.2(a), with dark lines representing the $40\mu\text{m}$ strips, impenetrable to the ions with $850\mu\text{m} \times 850\mu\text{m}$ transparent regions. Two sets of mutually perpendicular strips are employed which gives the appearance of a square mesh; the 200 MeV silver ions irradiate the mesh and the underlying Si(100) lattice perpendicular to the plane of the paper. The strips are so oriented with respect to the Si(100) face that one set are aligned parallel to the $\vec{g} = (220)$ direction during irradiation. When the same $\vec{g} = (220)$ vector is employed for XRT mapping the irradiated surface, Fig.2(b) results. The observed parallel lines are due to strain \vec{b}_1 developed at the irradiation interface, while the mutually perpendicular set of lines, which were also expected, do not appear as $\vec{g} \cdot \vec{b}_2 = 0$ for the selected vector. The proposed strain vectors \vec{b}_1 and \vec{b}_2 which explains this result are schematically drawn in Fig.2(a). When the same irradiated surface is selected for XRT mapping with another vector $\vec{g} = (040)$, the expected crossed lines appear (similar to the square mesh in Fig.2(a)) as $\vec{g} \cdot \vec{b} \neq 0$ for the strain vectors \vec{b}_1 and \vec{b}_2 . This is shown in Fig.2(c). It is to be noted here that an angle of 45° is included between $\vec{g} = (040)$ and $\vec{g} = (220)$. Also, the information presented here comes from a depth of $7\mu\text{m}$ as compared to the Ag ion range of $\sim 21\mu\text{m}$ in Si. Thus making the above effect originate from electronic loss ($S_e=12 \text{ MeV}/\mu\text{m}$).

The topographic results conclusively show appearance of strain perpendicular to an irradiated interface in regions subjected to electronic loss. Hence

a stress is associated with this strain whose origins are related to the irradiation event. As an irradiation interface is important here, any ion/target combination would yield similar results with varying extent of strain. We shall apply this result to explain irradiation induced changes in the resistivity plots (Fig.1) of Ni and Fe.

Polycrystalline materials in general and cold-rolled foils in particular contain a large number of stationary defects. We consider an edge dislocation as a representative case. In Fig.3 we show a situation where a lattice of 7 atoms continues as a 6-atom lattice, abruptly across an edge. This leaves a string of atoms, marked A, faced with a discontinuity. These atoms will however try to maintain its periodicity in the lattice and move towards one of the lines AX or AY. This will severely distort the lattice in this region. Under irradiation, the atom string A will be subjected to an irradiation interface and result in a stress $\vec{\tau}$, marked in Fig.3. An outcome of this could be a rearrangement of atoms near such a dislocation edge into new configurations. These configurations would be metastable in nature and will be sensed by a current which is driven during the rearrangement process. If stress $\vec{\tau}$ is sufficiently large, the entire string of atoms can be displaced to collect at grain boundaries. This could modify existing internal stress, as well as result in reorientation of grains [12].

In order to justify that these defects, arising out of irradiation are indeed associated with the microstructure of the material and distinct from the well known point defects, we show scaling of RV with various parameters in Fig.4. In Fig.4(a) we show RV vs irradiation time plots of cold-rolled Fe at two sample temperatures, $T = 300\text{K}$ and $T = 80\text{K}$ for an identical irradiation flux ($\sim 8.036 \times 10^8 \text{ ions cm}^{-2} \text{ sec}^{-1}$). $\Delta RV (= RV_{max} - RV_{t=0})$ which is a measure of the absolute amount of defects created and $\frac{\Delta RV}{RV}$, a quantity relative to the inherent defects at that temperature, works out to be $3.0333 \times 10^{-5}V$

and 0.035 at 300K and $5.25 \times 10^{-6}V$ and 0.037 at 80K. If RV originated due to point defects at room temperature, both ΔRV and $\frac{\Delta RV}{RV}$ would increase at 80K, due to increase in point defect density resulting from reduced defect mobility and hence slower recombination. But this is certainly not observed. It should also be noted that jumps in RV are missing at 80K. The ions employed here are 200 MeV Ag. But at 300K, the jumps are seen to be S_e (average value $\sim 15 \text{ MeV}/\mu\text{m}$ for Ag/Fe) related and ion independent (compare Figs.4(a) and 1(b)).

Fig.4(b) shows RV vs t plots for ion flux of $8.036 \times 10^8 \text{ ions cm}^{-2} \text{ sec}^{-1}$ and $1.384 \times 10^9 \text{ ions cm}^{-2} \text{ sec}^{-1}$ at room temperature. $\frac{\Delta RV}{RV}$ almost doubles which is consistent with larger dissipation in the latter, where the ions interact with a larger volume of microstructure. For a direct evidence on involvement of microstructure, RV of a cold-rolled foil is compared, under irradiation at room temperature, before and after annealing. Fig.4(c) shows the results. It is well known that annealing reduces stationary imperfections and a large volume of literature exists on this topic [12]. The effect on RV during irradiation of this annealed foil is a substantial reduction in this measured quantity. Hence reduction in microstructural defects is directly reflected in RV.

Having identified and verified the contribution of microstructural defects towards RV in the 4-probe measurement, we now proceed to analyse the features of Fig.1 in detail. The rise in RV with irradiation is a result of dissipation at the “internal surfaces” through formation of new atomic configurations or rearrangements under irradiation, as described in Fig.3. Similar reports of resistivity jumps have been assigned to atomic rearrangements in the literature [13]. The arrangements we report are not permanent but open to statistical decay. The levelling-off of RV at the jumps is then arising out of saturation in a quantity, which is the difference between production rate and decay rate of new configurations. These new configurations are randomly dis-

tributed in the material, under irradiation. As the production rate is constant during irradiation, it is a substantial increase in the decay rate which triggers these jumps. Considering each rearrangement to be equivalent to formation of one Frenkel pair (an underestimate, as several atoms can rearrange at dislocations/grain boundaries) and employing literature estimates of resistivity increase ($3000 \mu \Omega \text{ cm}$) for such pair formation [14] the average number of decay at the jumps turns out to be 1.968×10^{-2} . The contribution of each jump is about 6% of the total resistivity increase from beam-on to saturation. Such large decay rates at any given point during irradiation is not possible without positive feedback, where decay of some configurations induces other configurations to decay, limited only by the availability of such configurations.

Presence of positive feedback always opens the possibility for auto-oscillations which in this case would be periodic variations in rearrangement concentration and temperature. During the steady state, between beam-on and beam-off, such structures fill up the irradiation volume. On beam-off, these decay and is marked by steps in RV. Conceptually the release of such structures are similar to ones observed in neutron irradiated CH_4 [2], where heat had to be applied to observe them as the structures were frozen at low temperature (below 15K). In this experiment however, the structures are populated at room temperature and can be observed by simply switching off the irradiation source.

Finally, the above discussion of feedback assumes the microstructure to completely revert to its original configuration. This is however an ideal situation. In reality, complete reversal may not be achieved and reorientation of grains can result due to reasons already stated. We show in Fig.5a, θ - 2θ x-ray diffraction (XRD) scans for Ni. Comparing the XRD plots before irradiation (BF) and after irradiation (AF), it is clear that the higher order reflections increase in relative intensity. Also compared in the inset to this figure are step

scans of Ni for the (200) reflection. A systematic shift in the peak positions towards lower angles are recorded. Peak shifts in thin Ni films have been observed before, accompanied by increase in peak widths [15]. These were explained in terms of grain size variation. As we observe no variation in peak shape, the shifts in peak position reflect increase in lattice constant due to changes in existing internal stress; incorporation of solute(oxygen) atoms are ruled out as ion ranges far exceed Ni and Fe foil thicknesses. Another result obtained from XRD data of Fig.5 is an increase in relative intensity of all peaks towards higher angles. This is entirely an irradiation related effect and independent of the material under study or their initial relative peak intensity. These are assigned to texturing effects [12].

In conclusion, we have shown evidence of dissipative structure formation in metals under irradiation. These are formed as rearrangements in an already present microstructure filled with stationary imperfections like dislocations and grain boundaries. Employing topography we have identified the process leading to these rearrangements whose resistivity behaviour is similar to defect formation. We have also shown the presence of positive feedback during the process of irradiation and the resultant decay of irradiation induced structures, in one single experiment. The unmistakable participation of the microstructure in verifying the physical principles of positive feedback, under irradiation, has been established.

Acknowledgement: We acknowledge the cooperation extended by NSC, New Delhi, SSPL, Delhi and IUC, Indore during this study. Partial financial support from UGC is also acknowledged.

-
- [1] P.A. Selishchev & V.I. Sugakov, *Rad. Eff. Def. Sol.* 133, 237 (1995)
- [2] J.M. Carpenter, *Nature* 36, 358 (1987)
- [3] G. Nicolis and I. Prigogine, “Self Organisation in Non-equilibrium Systems”, Wiley, New York (1977)
- [4] H. Dammark et al., *Phil. Mag. Lett.* 67, 253 (1993)
- [5] A. Barbu et al., *Europhys. Lett.* 15, 3713 (1991)
- [6] S. Klaumunzer et al., *Phys. Rev. Lett.* 57, 850 (1986)
- [7] A. Dunlop et al., *Europhys. Lett.*, 15, 765 (1991) ; Z.G. Wang et al., *J. Phys. Condens. Matter*, 6, 6733 (1994)
- [8] A. Dunlop & D. Lesueur *Mat. Res. Soc. Symp. Proc.* 279, 51 (1993)
- [9] J. Marfaing et al., *Appl. Phys. Lett.* 57, 1739 (1990)
- [10] N. Hayashi et al. *Phys. Rev. Lett.* 70, 45 (1993)
- [11] B.B. Sharma et al., *MRS Proceedings on "Defects and Impurity Engineered Semiconductors and Devices"* Eds. S. Ashok et al., Vol. 378, 671 (1995)
- [12] C. Barrett & T.B. Massalski, “Structure of Metals”, 3rded., Macgraw-Hill, New York, pp 402 (1968)
- [13] T.N. Todorov & A.P. Sutton, *Phys. Rev. Lett.* 70, 2138 (1993)
- [14] F. Maury et al., *Phy. Rev. B* 14, 5303, 1976
- [15] X.D. Liu et al., *J. Phys. Condens. Matter* 6, L497 (1994)

Figure Captions

- Fig.1 : The response voltage (RV) generated during irradiation by a constant flux (5×10^9 ions $\text{cm}^{-2} \text{sec}^{-1}$) of 100 MeV oxygen ions in a 4-probe resistivity measurement setup. RV is plotted as a function of irradiation time interval (t) when the data was collected. All plots are normalised to RV at $t = 0$ for a particular current (I). (a) For Ni foils, the ion beam was switched on at $t = 0$ and switched off at $t = 380$; the inset shows one jump after beam off between $t = 386$ and $t = 406$. (b) For Fe foils, the ion beam was switched on at $t = 0$ and switched off at $t = 249$; the inset shows one jump just after beam on between $t = 22$ and $t = 52$

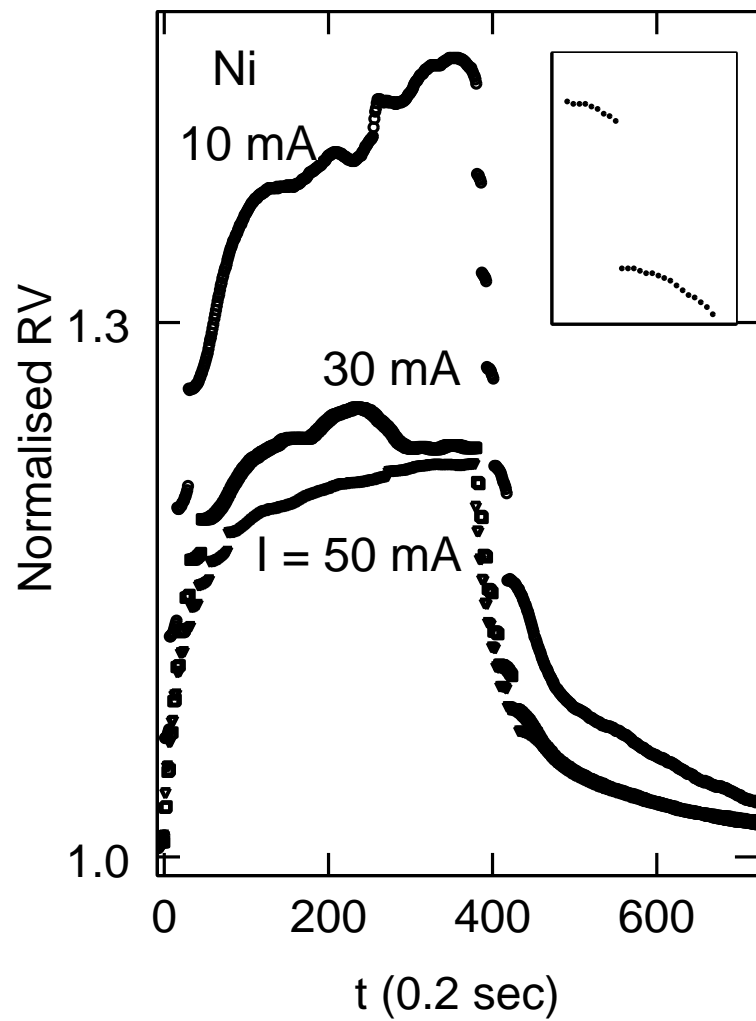
- Fig.2 : (a) Dark lines show two parallel sets of Ni wire strips, attached to each other after rotation by 90° . Each strip of square cross-section allows 200 MeV Ag ions to pass through the intermediate region and irradiate a Si(100) crystal below. The strips are so oriented with respect to Si(100) that one set, marked h, are parallel to its $\vec{g}(220)$. The strain vectors \vec{b}_1 and \vec{b}_2 are present on the Si surface in the configuration shown and are obtained from the XRT results. (b) XRT employing $\vec{g}(220)$, of Si(100) after irradiation; one set of lines disappear as $\vec{g} \cdot \vec{b}_2 = 0$ (c) XRT of the same employing $\vec{g}(040)$. Both sets of lines appear as $\vec{g} \cdot \vec{b} \neq 0$ for \vec{b}_1 and \vec{b}_2 .

- Fig.3 : Schematic diagram of dislocation edge and the effect of ion irradiation as derived from the XRT results (see text). The ions enter the plane of the paper.

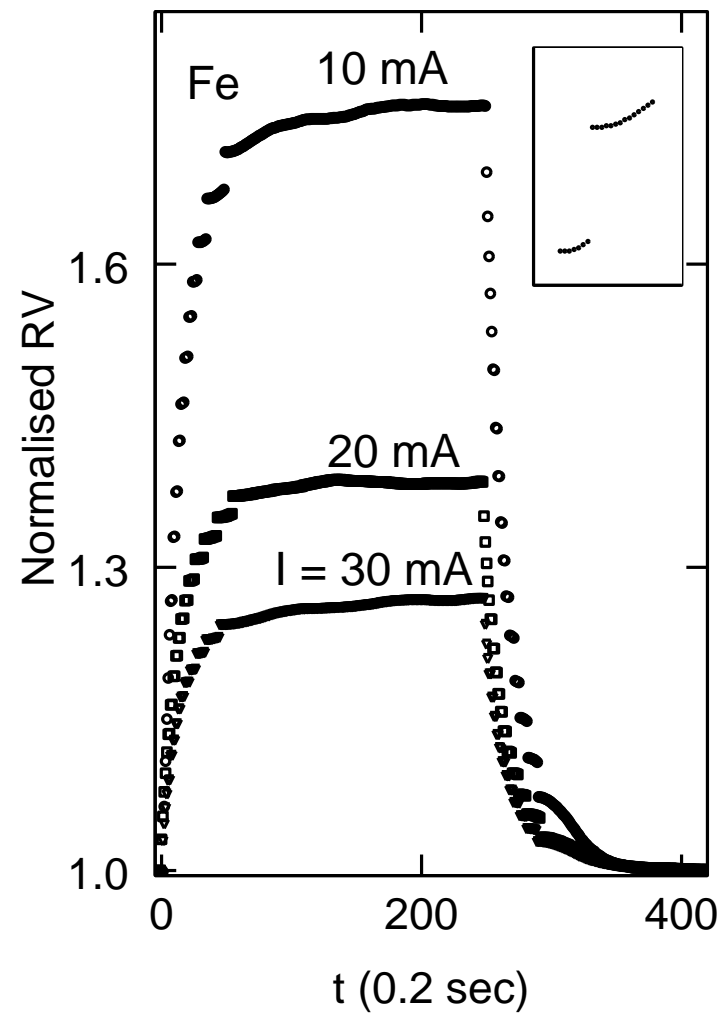
- Fig.4 : Effect on RV of an Fe foil is shown under various conditions. (a) Dependence on temperature, (b) dependence on the ion current and (c) dependence on annealing. This data is taken with 200 MeV Ag ions showing ion-independent behavior; $I = 100$ mA.

- Fig.5 : XRD plots before (BF) and after (AF) irradiation are compared. (a) For Ni foils showing changes in relative intensity ; inset shows details of the (200) reflections. (b) For Fe foils showing changes in relative intensity ; inset shows details of the (110) reflections.

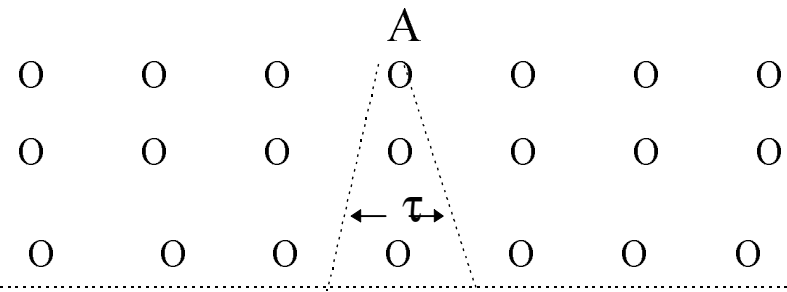
(a)



(b)

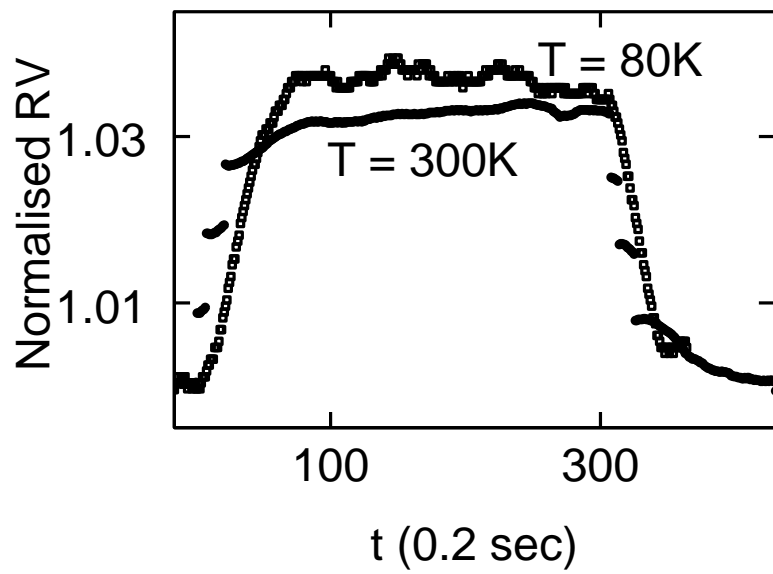


⊗ ION

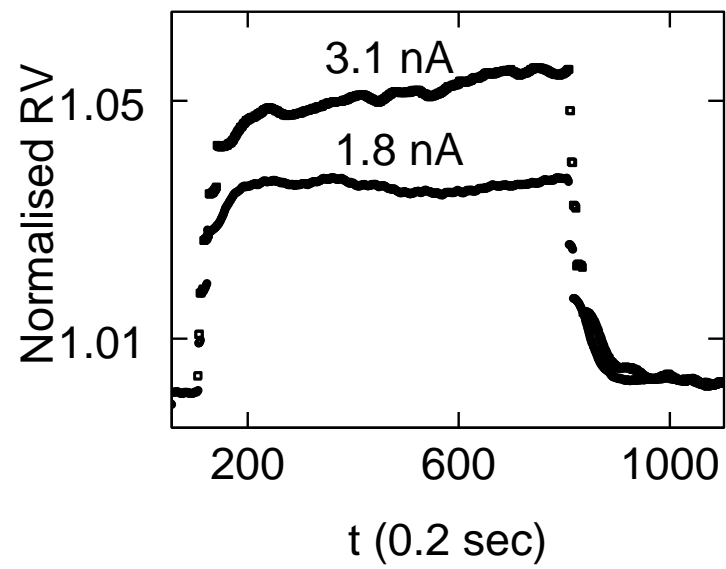


⊗ ION

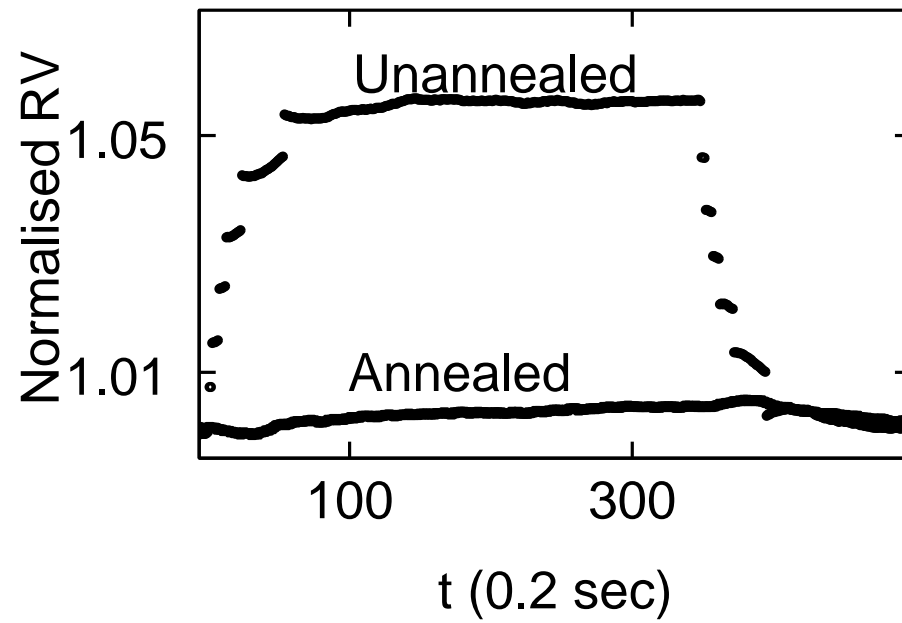
(a)



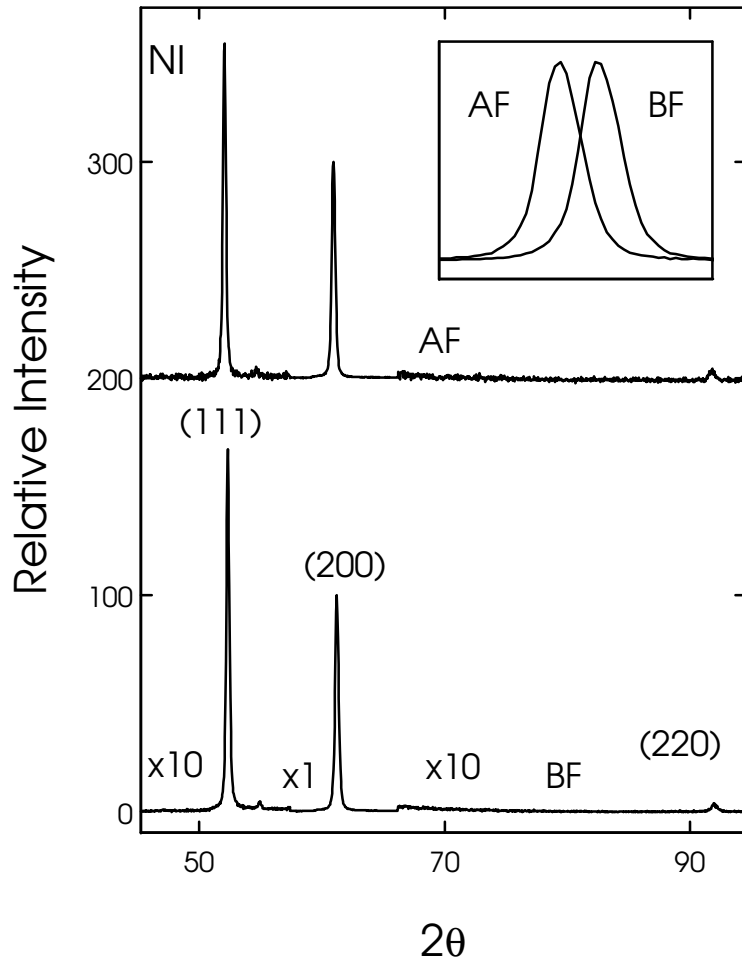
(b)



(c)



(a)



(b)

